JOURNAL OF SOLID STATE CHEMISTRY 50, 20–32 (1983)

Vacancy Diffusion in Magnetite–Hercynite Solid Solution

SHIGERU YAMAUCHI,* AKIO NAKAMURA, TOSHIAKI SHIMIZU, AND KAZUO FUEKI

Department of Industrial Chemistry, Faculty of Engineering, University of Tokyo, Hongo, Bunkyo-ku, Tokyo 113, Japan

Received February 23, 1983; in revised form June 14, 1983

To extend the chemical relaxation technique to ternary oxide systems, theoretical analysis was made to obtain an expression for the chemical diffusion coefficient in terms of the vacancy diffusion coefficient. An equation, $\tilde{D} = [C_O/(C_1 + C_2)]\, D_v(\frac{1}{2})(\partial \ln P(O_2)/\partial \ln C_v)$, was derived. This is similar to the one for the binary oxide system. Chemical relaxation experiments were made on the magnetite–hercynite solid solutions, $(Fe_{1-y}Al_y)_{3-\delta}O_4$ with $y = 0.0$, 0.067, 0.133, and 0.20, at temperatures between 1300 and 1400°C. The vacancy diffusion coefficient decreased remarkably with an increase in y. The activation energy was found to be 20.8 ± 3.7, 33.5 ± 4.2, 50.4 ± 3.6, and 66.3 ± 4.5 kcal/mole for $y = 0.0$, 0.067, 0.133, and 0.20, respectively. A strong dependence on y was also found. The dependence of the vacancy diffusion coefficient on y was interpreted to indicate that the jump frequency of cation vacancies is decreased by the introduction of aluminium ion.

Introduction

In most cases, metal deficit-type binary oxides have cation vacancies as major lattice defects and cation diffusion proceeds via vacancies. It is well known that the self-diffusion coefficient D_i of cations of kind i is related to the vacancy diffusion coefficient D_v by the equation (*1*)

$$D_i C_i = D_v C_v \tag{1}$$

where C_i and C_v denote the concentrations of cation i and vacancies, respectively. D_i is related to the tracer diffusion coefficient D_i^* by the equation

$$D_i f_0 = D_i^*, \tag{2}$$

where f_0 is the correlation factor. The chemical relaxation technique has been utilized for the measurement of the chemical diffusion coefficient $\tilde{D}$ in nonstoichiometric binary oxides. When a stepwise change of oxygen partial pressure is given to the system, physical properties depending on nonstoichiometric composition vary with time and finally reach new equilibrium values. If the surface reaction rate is high enough, the chemical diffusion coefficient $\tilde{D}$ can be calculated from the relaxation curve.

For chemical diffusion in binary oxides, Wagner (*2*) has derived the equation

$$\tilde{D} = (z_C D_C + |z_A| D_A) \frac{1}{|z_A|} \frac{C_C}{C_v} \left(\frac{1}{RT} \frac{\partial \mu_O}{\partial \ln C_v}\right) \tag{3}$$

where subscripts A and C denote anions and cations, respectively. C_C and C_v are concentrations of cations and vacancies, z_C and z_A are numbers of charge of both kinds

* To whom correspondence should be addressed.

0022-4596/83 $3.00

Copyright © 1983 by Academic Press, Inc.
All rights of reproduction in any form reserved.

of ions, and μ_O is the chemical potential of the oxygen atom.

If cation vacancy diffusion prevails in metal deficient binary oxides, $D_C \gg D_A$; therefore,

$$\tilde{D} = \frac{z_C C_C D_C}{|z_A| C_v} \frac{1}{2} \frac{\partial \ln P(O_2)}{\partial \ln C_v} = \frac{z_C D_v}{|z_A|} \frac{1}{2} \frac{\partial \ln P(O_2)}{\partial \ln C_v}. \quad (4)$$

Equation (4) indicates that the vacancy diffusion coefficient is directly determined from the chemical diffusion coefficient.

Chemical relaxation technique, applied to binary oxides such as CoO (*3, 4*), NiO (*3, 5*), and Fe_3O_4 (*6*), has demonstrated its relevance to obtaining vacancy diffusion coefficients. Although some papers have been published on chemical diffusion in ternary oxides (*7–9*), detailed theoretical analysis is needed. This paper aims to extend the chemical relaxation technique to ternary systems. For this purpose, the magnetite (Fe_3O_4)–hercynite ($FeAl_2O_4$) solid solution system was chosen, since the system has a wide nonstoichiometric range (*10–13*), and the chemical relaxation experiment was expected to be done by means of a thermobalance.

Theoretical

Phenomenological Theory of Chemical Relaxation in Ternary Oxide Systems

From the results of nonstoichiometry and tracer diffusion experiments on magnetite and magnetite–hercynite solid solutions at high oxygen pressures, it is considered that chemical diffusion proceeds by the cation diffusion via cation vacancies and oxide ions do not move (*10–16*). During the relaxation process after stepwise change in oxygen partial pressure, iron ions (Fe^{2+} and Fe^{3+}), Al^{3+} ions, and electrons diffuse in the same direction, while cation vacancies diffuse in the opposite direction.

Let us consider a slab equilibrated under an oxygen partial pressure, where the oxygen partial pressure is raised to a higher value at $t = 0$. If the surface reaction is fast enough, the surface has a nonstoichiometric composition in equilibrium with the new oxygen partial pressure. Cations migrate outwards to form a new oxide lattice. The cation diffusion flux J_M is proportional to the concentration gradient dC_M/dx, resulting in

$$J_M = -\tilde{D} \frac{dC_M}{dx}, \quad (5)$$

where D is the chemical diffusion coefficient. The weight change per unit area is proportional to cation flux $(J_M)_s$ at the surface:

$$\frac{dW}{dt} = g(J_M)_s = -g\tilde{D} \frac{dC_M}{dx} \quad (6)$$

where g denotes the weight of oxygen molecules per one mole of cation.

In magnetite–hercynite solid solutions, both iron ions and Al^{3+} ions diffuse via cation vacancies; thus,

$$J_M = J_1 + J_2 \quad (7)$$

$$\frac{dC_M}{dx} = \frac{dC_1}{dx} + \frac{dC_2}{dx} = -\frac{dC_v}{dx}, \quad (8)$$

where subscripts 1 and 2 denote iron ions and Al^{3+} ions, respectively. From Eqs. (5), (7), and (8),

$$J_M = J_1 + J_2 = \tilde{D} \frac{dC_v}{dx}. \quad (9)$$

Fluxes of iron ions, Al^{3+} ions, and electrons are expressed as follows:

$$J_1 = -\frac{D_1 C_1}{RT} \frac{d(\mu_1 + z_1 F\phi)}{dx} \quad (10)$$

$$J_2 = -\frac{D_2 C_2}{RT} \frac{d(\mu_2 + z_2 F\phi)}{dx} \quad (11)$$

$$J_3 = -\frac{D_3 C_3}{RT} \frac{d(\mu_3 + z_3 F\phi)}{dx}. \quad (12)$$

In Eqs. (10), (11), and (12), subscript 3 denotes electrons; μ_i and z_i are the chemical potential and the number of charges on species i; and ϕ is the electrical potential. Under equilibrium conditions,

$$\mu_1 + z_1\mu_3 = \mu_A \quad (13)$$

$$\mu_2 + z_2\mu_3 = \mu_B \quad (14)$$

$$N_A d\mu_A + N_B d\mu_B + N_O d\mu_O = 0 \quad (15)$$

where subscripts A, B, and O denote iron, aluminium, and oxygen atoms, respectively. N_A, N_B, and N_O are mole fractions of iron, aluminum, and oxygen, respectively.

Putting $z_3 = -1$ in Eq. (12) and utilizing Eqs. (13) and (14), Eqs. (10) and (11) are written

$$J_1 = -\frac{D_1C_1}{RT}\left(\frac{d\mu_A}{dx} + \frac{RTz_1J_3}{D_3C_3}\right) = -\frac{D_1C_1}{RT}\frac{d\mu_A}{dx} - \frac{D_1C_1z_1J_3}{D_3C_3} \quad (16)$$

$$J_2 = -\frac{D_2C_2}{RT}\left(\frac{d\mu_B}{dx} + \frac{RTz_2J_3}{D_3C_3}\right) = -\frac{D_2C_2}{RT}\frac{d\mu_B}{dx} - \frac{D_2C_2z_2J_3}{D_3C_3}. \quad (17)$$

Because of the high electronic conductivity of magnetite–hercynite solid solutions, D_3C_3 are much larger than D_1C_1 or D_2C_2. We see that the second terms on the right-hand side of Eqs. (16) and (17) are negligibly small, when compared to the first terms. Accordingly,

$$J_M = J_1 + J_2 = -\frac{D_1C_1}{RT}\frac{d\mu_A}{dx} - \frac{D_2C_2}{RT}\frac{d\mu_B}{dx}. \quad (18)$$

In the relaxation experiment, the change in nonstoichiometry is generally very small. Also, it is assumed as a first approximation that the molar ratio of Fe to Al remains constant during the relaxation run. As is shown in the Appendix, the chemical potential gradients are expressed by the equations

$$\frac{d\mu_A}{dx} = \left(-\frac{N_O}{N_A + N_B} - \frac{N_B\alpha}{N_A + N_B}\right)\frac{d\mu_O}{dx} \quad (19)$$

$$\frac{d\mu_B}{dx} = \left(-\frac{N_O}{N_A + N_B} + \frac{N_A\alpha}{N_A + N_B}\right)\frac{d\mu_O}{dx}. \quad (20)$$

Insertion of Eqs. (19) and (20) into J_M yields

$$J_M = \left(\frac{(D_1C_1 + D_2C_2)C_O}{RT(C_1 + C_2)} + \frac{C_1C_2(D_1 - D_2)\alpha}{RT(C_1 + C_2)(C_1 + C_2 + C_O)}\right)\frac{d\mu_O}{dx} = \left(\frac{(D_1C_1 + D_2C_2)C_O}{RT(C_1 + C_2)} + \frac{C_1C_2(D_1 - D_2)\alpha}{RT(C_1 + C_2)(C_1 + C_2 + C_O)}\right) \times \frac{RT}{C_v}\frac{1}{2}\frac{\partial \ln P(O_2)}{\partial \ln C_v}\frac{\partial C_v}{\partial x} \quad (21)$$

where

$$\alpha = \frac{N_O^2\delta\left(\frac{\partial \ln P(O_2)}{\partial y}\right)_\delta}{4(N_A + N_B)^2\left(\frac{\partial \ln P(O_2)}{\partial \ln \delta}\right)_y}. \quad (22)$$

Comparison of Eq. (21) with Eq. (9) yields

$$\tilde{D} = \left(\frac{(D_1C_1 + D_2C_2)C_O}{C_1 + C_2} + \frac{C_1C_2(D_1 - D_2)\alpha}{(C_1 + C_2)(C_1 + C_2 + C_O)}\right) \times \frac{1}{2C_v}\frac{\partial \ln P(O_2)}{\partial \ln C_v}. \quad (23)$$

If the second term in parenthesis in Eq. (23) is much smaller than the first term,

$$\tilde{D} = \frac{(D_1C_1 + D_2C_2)C_O}{(C_1 + C_2)C_v} \times \left(\frac{1}{2}\frac{\partial \ln P(O_2)}{\partial \ln C_v}\right). \quad (24)$$

When either C_1 or C_2 approaches zero, Eq. (24) coincides with Eq. (4).

Vacancy Diffusion Coefficient in Ternary Oxide System

Manning (*18*) has derived an equation expressing the correlation factor of interdiffusion by the vacancy mechanism in a binary alloy system. According to Manning,

$$D_i^* = (\tfrac{1}{6})l^2x_v\omega_i f_i \quad (25)$$

$$D_v = (\tfrac{1}{6})l^2(x_1\omega_1 f_1 + x_2\omega_2 f_2)/f_0 \quad (26)$$

$$= (x_1D_1^* + x_2D_2^*)/x_v f_0, \quad (27)$$

where l is the jump distance, ω_1 and ω_2 are the vacancy-atom exchange rates for the two kinds of atoms, f_0 is the correlation factor of tracer diffusion. x_1, x_2, and x_v are mole fractions of metals 1, 2, and vacancy, respectively. f_1 and f_2 are the correlation factors of metals 1 and 2. Manning's expression for f_1 is

$$f_1 = \frac{M_0(x_1\omega_1 f_1 + x_2\omega_2 f_2)/f_0}{2\omega_1 + M_0(x_1\omega_1 f_1 + x_2\omega_2 f_2)/f_0}, \quad (28)$$

where M_0 is defined by

$$M_0 = \frac{2f_0}{1 - f_0}. \quad (29)$$

An equation similar to (28) holds for f_2.

Manning's equation was originally derived for interdiffusion in binary alloys. Equations (25)–(28) were applied to interdiffusion in the NiO–CoO system by Chen and Peterson (*19*) and by Dieckmann and Schmalzried (*7*). If oxide ions are actually immobile in the ternary oxide system, Eq. (26) holds; hence, one can obtain an equation for the vacancy diffusion coefficient in ternary oxide systems. Rewriting Eq. (27) with the aid of Eq. (2) results in

$$D_v = (x_1D_1 + x_2D_2)/x_v \quad (30)$$

or

$$C_vD_v = C_1D_1 + C_2D_2. \quad (31)$$

Equation (31) is an extension of Eq. (1) to ternary oxides. Insertion of Eq. (31) into Eq. (24) yields

$$\tilde{D} = -\frac{C_OD_v}{C_1 + C_2}\frac{1}{2}\frac{\partial \ln P(O_2)}{\partial \ln C_v}. \quad (32)$$

When C_1 or C_2 approaches zero, the right-hand side of Eq. (32) coincides with that of Eq. (4). Equation (32) gives a relevant relationship to be utilized in calculating vacancy diffusion coefficients from measured chemical diffusion coefficients.

Experimental

Materials

Magnetite–hercynite solid solutions were prepared by the same method as reported previously in Ref. (*13*). Sintered specimens were used for the measurement of nonstoichiometry and single crystals were employed for the measurement of the chemical diffusion coefficient. Single crystals, 5 mm in diameter and 100 mm in length, were grown by the floating zone method, utilizing a xenon arc image furnace. Rectangular or cylindrical specimens, about 1 g in weight, were cut from the single crystals.

Measurements

Nonstoichiometry and chemical relaxation were studied by means of a thermobalance. Details are described elsewhere (*6*). Nonstoichiometry was determined from the equilibrium weight of the specimen. Chemical relaxation was studied by following the weight change after the abrupt change in the total pressure of an $Ar–O_2$ gas mixture. A preliminary experiment was conducted

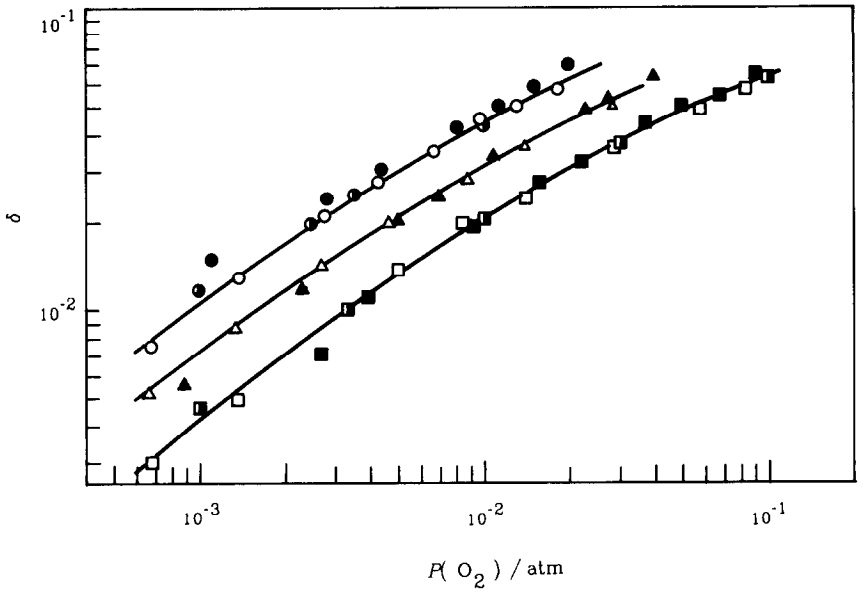

FIG. 1. Nonstoichiometry in $Fe_{3-\delta}O_4$. Present results: ○, 1300°C; △, 1350°C; □, 1400°C. Recalculated from the data of Nakamura *et al.* (*6*): ●, 1300°C; ▲, 1350°C; ■, 1400°C. Dieckmann (*20*): ◑, 1300°C; ◨, 1400°C.

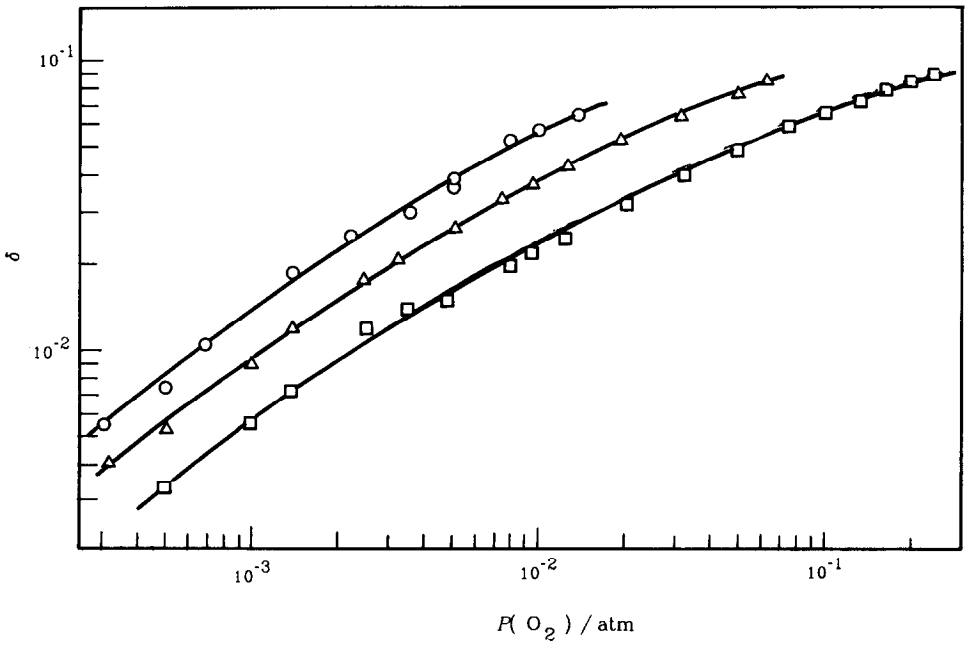

FIG. 2. Nonstoichiometry in $(Fe_{0.933}Al_{0.067})_{3-\delta}O_4$. ○, 1300°C; △, 1350°C; □, 1400°C.

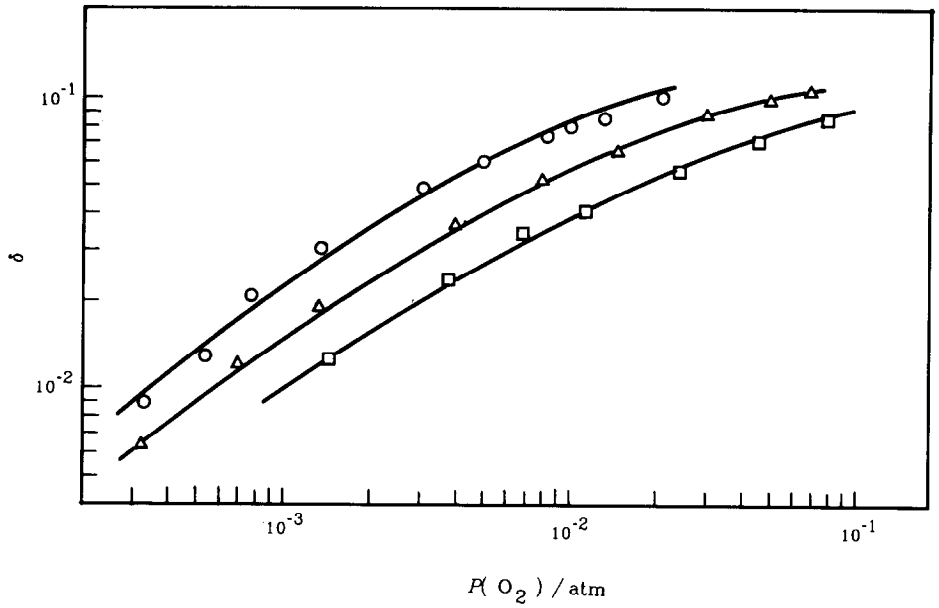

FIG. 3. Nonstoichiometry in $(Fe_{0.866}Al_{0.133})_{3-\delta}O_4$. ○, 1300°C; △, 1350°C; □, 1400°C.

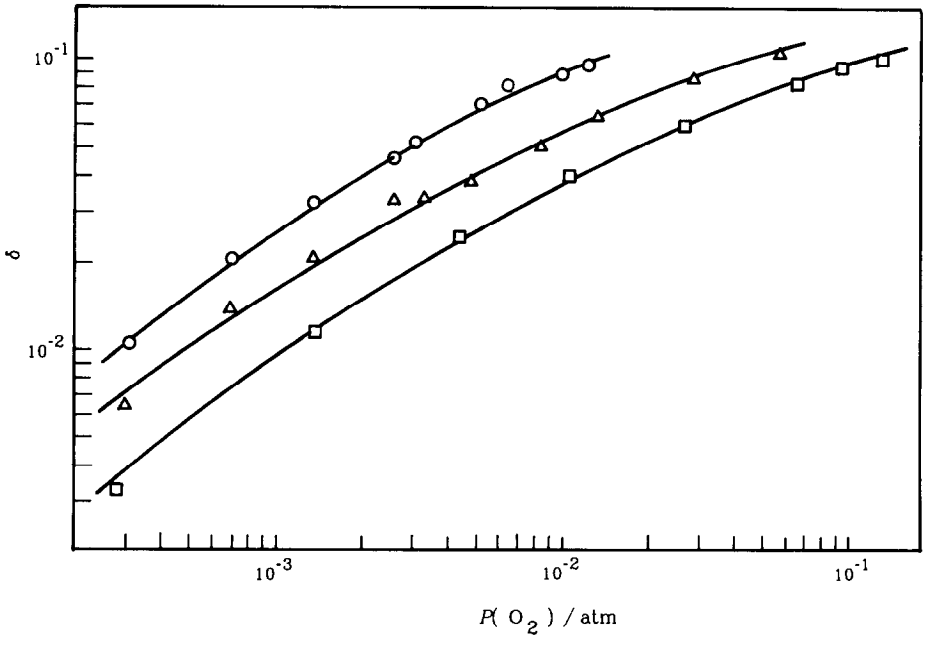

FIG. 4. Nonstoichiometry in $(Fe_{0.8}Al_{0.2})_{3-\delta}O_4$. ○, 1300°C; △, 1350°C; □, 1400°C.

to establish corrections for buoyancy and thermomolecular force.

Results

Nonstoichiometry

The metal-to-oxygen atomic ratio of magnetite and magnetite–hercynite solid solution changes from metal deficit to metal excess with decreasing oxygen pressures. An inflection point is expected at the stoichiometric composition, in the plot of weight vs log $P(O_2)$ (*16, 20*). In this study, measurements were made more carefully than previously (*6, 13*) and inflection points were observed for each isotherm curve at $10^{-4.5}$ to 10^{-7} atm, depending on temperature and the hercynite concentration. The stoichiometric composition was determined from the inflection point. Results for cation deficient composition ranges are summarized in Figs. 1 to 4. In our previous paper (*6*), nonstoichiometry was calculated, assuming that magnetite in coexistence with wuestite has the stoichiometric composition. Therefore, the previously reported data were recalculated, using the new stoichiometric points. They are also reported in Fig. 1. The nonstoichiometric data for magnetite, recently reported by Dieckmann (*20*), are also plotted in the same figure. All three data are in good agreement. The value of the nonstoichiometry parameter δ for magnetite–hercynite solid solutions increased with decreasing temperature and increasing hercynite concentration. This dependence of δ on temperature and hercynite concentration is similar to that reported elsewhere (*13*).

Chemical Relaxation

Figure 5 shows typical relaxation curves. Solving Eq. (6) for the three-dimensional case, one obtains

$$\frac{W(t) - W(0)}{W(\infty) - W(0)} = \frac{\int_V [C_M(r,t) - C_M^0]dr}{V(C_M^\infty - C_M^0)}. \quad (33)$$

Green's theorem is utilized in the integration; r is the vector indicating the position in the sample specimen; C_M^0 and C_M^∞ are the concentrations at $t = 0$ and ∞, respectively. $C_M(r,t)$ is the cation concentration at time t and position r.

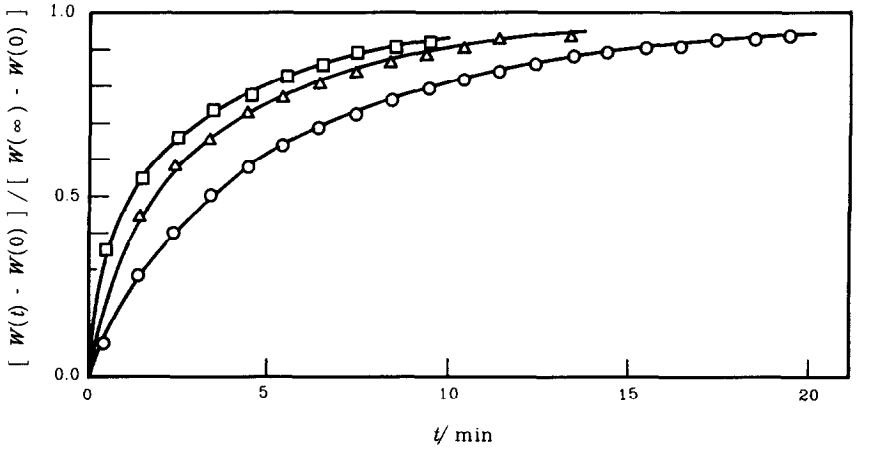

FIG. 5. Oxidation relaxation curves for $(Fe_{0.933}Al_{0.067})_{3-\delta}O_4$. ○, 1300°C, from $\delta = 0.010$ to 0.018; △, 1350°C, from $\delta = 0.010$ to 0.017; □, 1400°C, from $\delta = 0.010$ to 0.017.

Solution of Eq. (33) for a rectangular specimen of dimensions $2l_1 \times 2l_2 \times 2l_3$ is

$$\frac{W(t) - W(0)}{W(\infty) - W(0)} = \frac{512}{\pi^6} \prod_{i=1}^{3} \sum_{n_i=0}^{\infty} \frac{\exp[-\tilde{D}t\{(2n_i + 1)\pi/2l_i\}^2]}{(2n_i + 1)^2} \quad (34)$$

and that for a cylindrical specimen of radius a and length $2l$ is

$$\frac{W(t) - W(0)}{W(\infty) - W(0)} = \frac{32}{\pi^2 a^2} \sum_{n=0}^{\infty} \frac{\exp[-\tilde{D}t\{(2n + 1)\pi/2l\}^2]}{(2n + 1)^2} \times \sum_{m=0}^{\infty} \frac{\exp(-\tilde{D}t\alpha_m^2)}{\alpha_m^2}. \quad (35)$$

In Eq. (35) α_m is the mth positive root of

$$J_0(a\alpha_m) = 0,$$

where J_0 is the Bessel function of zero order.

To obtain accurate $\tilde{D}$ value, the right-hand side of Eqs. (34) and (35) are computed as a function of $\tilde{D}t$. Using the table of $[W(t) - W(0)]/[W(\infty) - W(0)]$ vs $\tilde{D}t$, $\tilde{D}t$ was determined from the observed weight change. $\tilde{D}t$ was then plotted against t. If the relaxation process is diffusion-controlled, this plot should give a straight line. Figure 6 shows the plot of $\tilde{D}t$ vs t. The plots for oxidation and reduction runs are straight and give the same slope. It is concluded that the reaction is diffusion-controlled.

A small dependence of $\tilde{D}$ on oxygen pressure was also found, as in the case of magnetite (*6*). D_v was calculated by using Eq. (32) with the aid of the nonstoichiometric data of Figs. 1–4. The oxygen pressure dependence was not found for calculated D_v values within experimental error, as is illustrated in Table I.

Table II summarizes D_v values and Fig. 7 shows Arrhenius plots for D_v. D_v decreases with the increase in hercynite content. Vacancy diffusion coefficients of magnetite, reported in the previous paper (*6*), are also

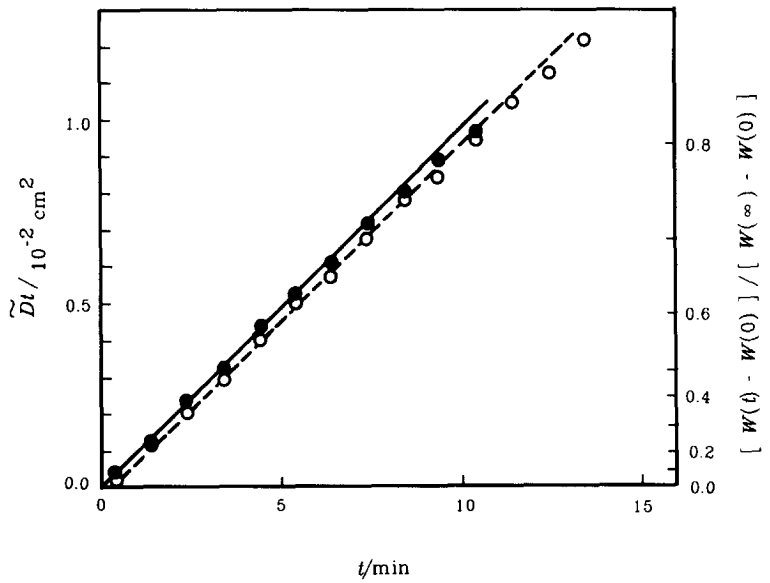

FIG. 6. $\tilde{D}t$ vs t plots for $(Fe_{0.933}Al_{0.067})_{3-\delta}O_4$ at 1350°C. ●, oxidation run; ○, reduction run.

TABLE I

OBSERVED CHEMICAL DIFFUSION COEFFICIENTS AND CALCULATED VACANCY DIFFUSION COEFFICIENTS FOR $(Fe_{0.8}Al_{0.2})_{3-\delta}O_4$ AT 1300°C

P_I[a] (10^{-3} atm)	P_{II}[a] (10^{-3} atm)	$\tilde{D}$ (10^{-6} cm^2 sec^{-1})	$\partial \ln \delta / \partial \ln P(O_2)$	D_v (10^{-6} cm^2 sec^{-1})
2.71	1.11	1.255	0.634	1.193
1.11	2.71	1.317	0.634	1.252
5.84	2.34	1.993	0.543	1.622
2.34	5.84	2.150	0.543	1.750
5.84	2.34	1.539	0.543	1.252
7.24	17.7	3.20	0.349	1.685
17.7	7.24	2.591	0.349	1.356

[a] P_I and P_{II} are the oxygen partial pressures before and after the change in the oxygen pressures, respectively.

plotted in the same figure. Present results are about two times larger than the previous ones. The discrepancy is attributed to the differences in the method of determining $\tilde{D}$ and the sizes of the specimens.

In the previous paper (*6*), $\tilde{D}$ is determined from the slope of the plot of $\log[1 - \{W(t) - W(0)\}/\{W(\infty) - W(0)\}]$ vs, t. Such a plot gives a linear relation only in the range of $\{W(t) - W(0)\}/\{W(\infty) - W(0)\} > 0.6$. Moreover, the data in the range of $\{W(t) - W(0)\}/\{W(\infty) - W(0)\} > 0.9$ contain a large relative error. Therefore, the method employed in the previous paper gives $\tilde{D}$ value with considerable errors. The present method utilizes the whole data of $\{W(t) - W(0)\}/\{W(\infty) - W(0)\} < 0.8$. Therefore, more accurate $\tilde{D}$ values are obtained. In the previous work, a rectangular magnetite specimen of 2.52 × 3.95 × 10.61 mm was used. The sample used in the present experiment is in a cylindrical form, 5.35 mm in diameter and 15.08 mm in length. When the specimen is small, the edge effect seems remarkable. Moreover, when the weight change is large in the relaxation runs, errors in the measurements are small. Therefore, the present result should be more accurate than the previous ones.

TABLE II

VACANCY DIFFUSION COEFFICIENTS IN $(Fe_{1-y}Al_y)_{3-\delta}O_4$[a]

	D_v (10^{-6} cm^2 sec^{-1})		
y	1300°C	1350°C	1400°C
0.0	11.62 ± 0.5	13.3 ± 0.5	17.3 ± 0.7
0.0667	7.46 ± 0.03	11.0 ± 0.4	13.4 ± 0.7
0.133	3.26 ± 0.1	4.53 ± 0.2	8.2 ± 0.2
0.2	1.44 ± 0.09	3.31 ± 0.08	5.17 ± 0.1

[a] Figures following ± are the standard deviations of the mean.

Discussion

Activation Energy of Vacancy Diffusion Coefficient

Table III shows the activation energy E_v and the pre-exponential factor D_v^0 for the vacancy diffusion coefficient D_v. Activation energies are plotted in Fig. 8. Figure 8 clearly indicates that the activation energy depends markedly on Al^{3+} content.

Halloran and Bowen (*16*) have reported that the activation energies Q of D^*_{Fe} are −37.2, −21.4, and 0 kcal/mole for $y = 0.0$, 0.163, and 0.323, respectively, assuming temperature independence of f_1. The activation energy for the vacancy jump frequency into iron sites E'_v, can be calculated

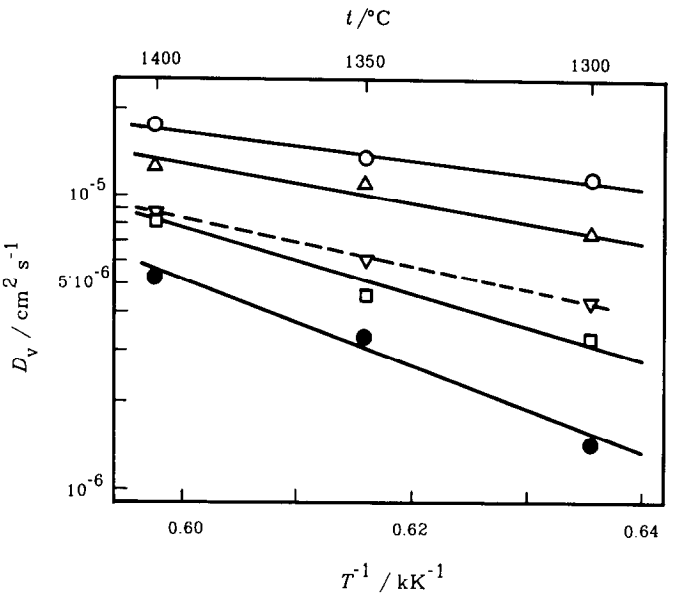

FIG. 7. Arrhenius plots of vacancy diffusion coefficients in $(Fe^{*}_{1-y}Al_y)_{3-\delta}O_4$. ○, $y = 0$; △, $y = 0.067$; □, $y = 0.133$; ●, $y = 0.2$; ▽, $y = 0$ (Nakamura *et al.* (*6*)).

from the above Q values by using the following equation:

$$E'_v = R\left(\frac{\partial \ln \omega_1}{\partial(1/T)}\right)_{P_{O_2}} = R\left(\frac{\partial \ln D^*_{Fe}}{\partial(1/T)}\right)_{P_{O_2}} - R\left(\frac{\partial \ln x_v}{\partial(1/T)}\right)_{P_{O_2}} = Q - E_s \quad (36)$$

where E_s is the enthalpy change due to dissolution of oxygen at constant oxygen pressures. E'_v coincides with E_v at $y = 0$.

The value of E_s, obtained from the nonstoichiometric data of Figs. 1–4, is −48 kcal/mole, irrespective of the Al^{3+} ion content, whereas the value of E_s, derived from recent data for nonstoichiometric magnetite reported by Dieckmann (*20*), is −49.4 kcal/mole. Using $E_s = -48$ kcal/mole and Q values described above, values of E'_v were calculated. The results are also plotted in Fig. 8. It is seen that E'_v increases with the increase in y. The increase of activation energy of D_v and ω_1 implies that the vacancy jump is retarded by the addition of Al^{3+} ions.

TABLE III

ARRHENIUS PARAMETERS FOR VACANCY DIFFUSION IN $(Fe_{1-y}Al)_{3-\delta}O_4$

y	$\ln(D^0_v)$ (cm² sec⁻¹)	E_v (kcal/mole⁻¹)
0.0	−4.72 ± 1.1	20.8 ± 3.7
0.0667	−1.09 ± 1.3	33.5 ± 4.2
0.133	3.2 ± 1.1	50.4 ± 3.6
0.2	7.8 ± 1.4	66.3 ± 4.5

A similar calculation was made on the activation energy of D^*_{Fe} in magnetite reported by Dieckmann and Schmalzried (*15*). The result is also plotted in Fig. 8 and shows a fair agreement with the present result.

Dependence of Vacancy Diffusion on Hercynite Concentration

Values of D_v in Table II show strong dependence on the mole fraction y of Al^{3+} ions in cations. To show the dependence of

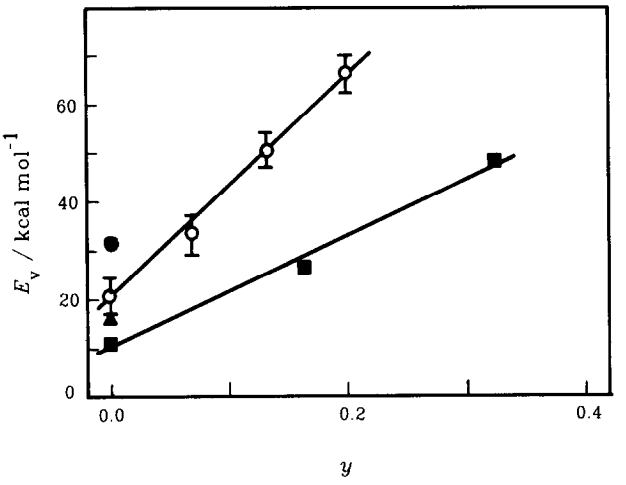

FIG. 8. Activation energy of vacancy diffusion in $(Fe_{1-y}Al_y)_{3-\delta}O_4$. ○, this work; ▲, calculated from Dieckmann and Schmalzried (*15*); ■, calculated from Halloran and Bowen (*16*); ●, Nakamura *et al.* (*6*).

D_v on y more clearly, $D_v/D_v(0)$ plotted against y is shown in Fig. 9. According to Eq. (26), the dependence of D_v on y is given by

$$\frac{D_v(y)}{D_v(0)} = \frac{x_1\omega_1 f_1 + x_2\omega_2 f_2}{\omega_1^0 f_0}$$

$$= \frac{\omega_1 f_1 + (\omega_2 f_2 - \omega_1 f_1)y}{\omega_1^0 f_0}$$

$$= [1 + \{(f_2/f_1)\gamma - 1\}y] \times (f_1/f_0)(\omega_1/\omega_1^0), \quad (37)$$

where ω_1^0 denotes the vacancy jump frequency in magnetite. Plots in Fig. 8 show that D_v decreases with increase of y. Therefore, $\omega_2 f_2$ is smaller than $\omega_1 f_1$. This implies that D^*_{Al} is smaller than D^*_{Fe} in the magnetite–hercynite system.

From Eqs. (28) and (29), the following equation is obtained:

$$f_1 = 1 - \frac{1 - f_0}{x_1 + x_2(f_2/f_1)\gamma}, \quad (38)$$

where γ is ω_2/ω_1, the ratio of the jump frequency. An expression for f_2 bears similarity to Eq. (28) and leads to the following equation:

$$f_2 = 1 - \frac{(1 - f_0)(f_2/f_1)\gamma}{x_1 + x_2(f_2/f_1)\gamma}. \quad (39)$$

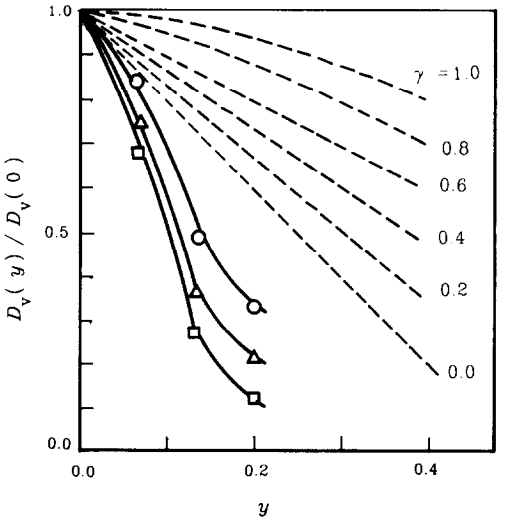

FIG. 9. Dependence of D_v on y. ○, 1300°C; △, 1350°C; □, 1400°C. The broken lines are the ones calculated by Eq. (41).

From Eqs. (38) and (39) an equation for f_2/f_1 is derived:

$$\frac{f_2}{f_1} = \frac{-[(f_0 - x_2)(1 - \gamma) + 1] + \sqrt{[(f_0 - x_2)(1 - \gamma) + 1]^2 + 4x_2\gamma}}{2x_2\gamma}. \quad (40)$$

Insertion of Eq. (39) into Eq. (37) gives

$$\frac{D_v(y)}{D_v(0)} = [1 + \{(f_2/f_1)\gamma - 1\}(y/f_0)](\omega_1/\omega_1^0). \quad (41)$$

Assuming that ω_1 is constant and equal to ω_1^0, the right-hand side of Eq. (41) was calculated for several values of γ by using Eq. (40) for calculation of f_2/f_1. The results are given by broken lines in Fig. 9. The solid lines in Fig. 9 are below the broken lines. This fact leads to the conclusion that the frequency of vacancy jumps into iron sites decreases with the increase in y. This is consistent with the conclusion in the preceding section verifying that the vacancy jump is retarded by addition of Al^{3+} ions. However, it is not possible to discuss the detailed mechanism of this effect at the present time.

Appendix: Driving Force in the Chemical Relaxation in Ternary Metal Oxides

In the chemical relaxation experiment on solid solutions of two oxides $(A_{1-y}B_y)_mO_n$, the driving force of diffusion is given by the gradient of the chemical potential of oxygen. However, when oxide ions form a rigid sublattice and the chemical relaxation process is described by the diffusion of cations within the cation sublattice, the flux of both cations is determined by the gradient of the electrochemical potential of the cations, as given by Eqs. (10) and (11). With the aid of thermodynamic relations and some appropriate assumptions, the driving forces are expressed in terms of the gradient of the chemical potentials of neutral A and B atoms, as shown in Eqs. (19) and (20).

In the chemical relaxation runs, changes in the metal-to-oxygen ratio is small. It is assumed that the atomic ratio of A and B remains constant. The Gibbs–Duhem equation is used for this purpose:

$$N_A d\mu_A + N_B d\mu_B + N_O d\mu_O = 0, \quad (A\text{-}1)$$

where N_A, N_B, and N_O are the mole fractions. Equation (A-1) can be rewritten as

$$d\mu_A = -\frac{N_B}{N_A} d\mu_B - \frac{N_O}{N_A} d\mu_O. \quad (A\text{-}2)$$

As Eq. (A-2) is perfect differential, the following relation holds (*21*):

$$\left(\frac{\partial(N_O/N_A)}{\partial\mu_B}\right)_{\mu_O} = \left(\frac{\partial(N_B/N_A)}{\partial\mu_O}\right)_{\mu_B} = \frac{-\left(\frac{\partial\mu_B}{\partial\mu_O}\right)_{N_B/N_A}}{\left(\frac{\partial\mu_B}{\partial(N_B/N_A)}\right)_{\mu_O}}.$$

Therefore,

$$\left(\frac{\partial\mu_B}{\partial\mu_O}\right)_{N_B/N_A} = -\left(\frac{\partial(N_O/N_A)}{\partial\mu_B}\right)_{\mu_O}\left(\frac{\partial\mu_B}{\partial(N_B/N_A)}\right)_{\mu_O} = -\left(\frac{\partial(N_O/N_A)}{\partial(N_B/N_A)}\right)_{\mu_O} = -\frac{N_O}{1 - N_O} - \frac{1}{N_A(1 - N_O)}\left(\frac{\partial N_O}{\partial(N_B/N_A)}\right)_{\mu_O} \quad (A\text{-}3)$$

The final factor in Eq. (A-3) is rewritten as

$$\left(\frac{\partial N_O}{\partial(N_B/N_A)}\right)_{\mu_O} = -\frac{\left(\frac{\partial\mu_O}{\partial(N_B/N_A)}\right)_{N_O}}{\left(\frac{\partial\mu_O}{\partial N_O}\right)_{(N_B/N_A)}}. \quad (A\text{-}4)$$

By expressing the mole fraction of B with

the variable y, the numerator in Eq. (A-4) is converted to

$$\left(\frac{\partial \mu_O}{\partial (N_B/N_A)}\right)_{N_O} = \left(\frac{\partial \mu_O}{\partial y}\right)_\delta \left(\frac{\partial y}{\partial (N_B/N_A)}\right)_\delta = \frac{1}{2} RT \left(\frac{\partial \ln P(O_2)}{\partial y}\right)_\delta \left(\frac{N_A}{N_A + N_B}\right)^2.$$

The denominator in Eq. (A-4) is written as

$$\left(\frac{\partial \mu_O}{\partial N_O}\right)_{(N_B/N_A)} = \left(\frac{\partial \mu_O}{\partial \ln \delta}\right)_y \left(\frac{\partial \ln \delta}{\partial \delta}\right)_y \left(\frac{\partial \delta}{\partial N_O}\right)_y = \frac{1}{2} RT \left(\frac{\partial \ln P(O_2)}{\partial \ln \delta}\right)_y \frac{1}{\delta} \frac{4}{N_O^2}.$$

Utilizing the above relations, Eq. (A-3) yields the following expression for the gradient of the chemical potential of B:

$$\left(\frac{\partial \mu_B}{\partial x}\right)_{(N_B/N_A)} = \left[-\frac{N_O}{1 - N_O} + \frac{N_A N_O^2 \delta}{4(N_A + N_B)^3} \times \frac{\left(\frac{\partial \ln P(O_2)}{\partial y}\right)_\delta}{\left(\frac{\partial \ln P(O_2)}{\partial \ln \delta}\right)_y} \right] \left(\frac{\partial \mu_0}{\partial x}\right)_{(N_B/N_A)}$$

$$= \left(-\frac{N_O}{N_A + N_B} + \frac{N_A \alpha}{N_A + N_B} \right) \times \left(\frac{\partial \mu_O}{\partial x}\right)_{(N_B/N_A)}, \quad \text{(A-5)}$$

where α is defined by

$$\alpha = \frac{N_O^2 \delta}{4(N_A + N_B)^2} \frac{\left(\frac{\partial \ln P(O_2)}{\partial y}\right)_\delta}{\left(\frac{\partial \ln P(O_2)}{\partial \ln \delta}\right)_y}.$$

Similar relation can be derived for the gradient of the chemical potential of A.

$$\frac{d\mu_A}{dx} = \left(-\frac{N_O}{N_A + N_B} - \frac{N_B \alpha}{N_A + N_B} \right) \left(\frac{d\mu_O}{dx}\right)_{(N_B/N_A)}. \quad \text{(A-6)}$$

Equations (A-6) and (A-5) express the driving force on A and B ions, in a chemical relaxation experiment on ternary oxides.

References

1. P. G. SHEWMON, "Diffusion in Solids," p. 53, McGraw–Hill, New York, 1963.
2. C. WAGNER, *Z. Phys. Chem. Abt. B* **11,** 139 (1930); *Z. Phys. Chem. Abt. B* **32,** 447 (1936).
3. J. B. PRICE AND J. B. WAGNER, JR., *Z. Phys. Chem. N.F.* **49,** 257 (1966).
4. J. WIMMER, R. N. BLUMENTHAL, AND I. BRANSKY, *J. Phys. Chem. Solids* **36,** 269 (1975).
5. J. DEREN AND S. MROWEC, *J. Mater. Sci.* **8,** 545 (1973).
6. A. NAKAMURA, S. YAMAUCHI, K. FUEKI, AND T. MUKAIBO, *J. Phys. Chem. Solids* **39,** 1203 (1978).
7. R. DIECKMANN AND H. SCHMALZRIED, *Ber. Bunsenges.* **79,** 1108 (1975).
8. A. E. PALADINO, L. G. RUBIN, AND J. S. WAUGH, *J. Phys. Chem. Solids* **26,** 391 (1965).
9. D. B. SCHWARZ AND H. U. ANDERSON, *J. Electrochem. Soc.* **122,** 707 (1975).
10. B. D. ROITER, *J. Amer. Ceram. Soc.* **47,** 509 (1964).
11. T. O. MASON AND H. K. BOWEN, *J. Amer. Ceram. Soc.* **64,** 86 (1981).
12. A. PETRIC, K. T. JACOB, AND C. B. ALCOCK, *J. Amer. Ceram. Soc.* **64,** 632 (1981).
13. A. NAKAMURA, S. YAMAUCHI, AND K. FUEKI, *Bull. Chem. Soc. Japan* **52,** 1019 (1979).
14. R. DIECKMANN AND H. SCHMALZRIED, *Z. Phys. Chem. N.F.* **96,** 331 (1975).
15. R. DIECKMANN AND H. SCHMALZRIED, *Ber. Bunsenges.* **81,** 344 (1977).
16. J. W. HALLORAN AND H. K. BOWEN, *J. Amer. Ceram. Soc.* **63,** 45 (1980).
17. N. L. PETERSON, W. K. CHEN, AND D. WOLF, *J. Phys. Chem. Solids* **41,** 709 (1980).
18. J. R. MANNING, "Diffusion Kinetics for Atoms in Crystals," p. 125, Van Nostrand, Princeton, N.J., 1968.
19. W. K. CHEN AND N. L. PETERSON, *J. Phys. Chem. Solids* **34,** 1093 (1973).
20. R. DIECKMANN, *Ber. Bunsenges.* **86,** 112 (1982).
21. G. N. LEWIS AND M. RANDALL (revised by K. S. Pitzer and L. Brewer), "Thermodynamics," p. 557, McGraw–Hill, New York, 1961.